Synthesis and Structural Comparison of a Series of Divalent $Ln(Tp^{R,R'})_2$ (Ln = Sm, Eu, Yb) and Trivalent $Sm(Tp^{Me_2})_2X$ (X = F, Cl, I, BPh_4) Complexes

Anna C. Hillier,[#] XingWang Zhang,[†] Graham H. Maunder,[#] Sung Ying Liu,[#] Todd A. Eberspacher,[‡] Mathew V. Metz,[‡] Robert McDonald,[†] Ângela Domingos,[§] Noémia Marques,[§] Victor W. Day,[‡] Andrea Sella,*[,#] and Josef Takats*[,†]

Department of Chemistry, University of Alberta, Edmonton, AB, Canada T6G 2G2, Christopher Ingold Laboratories, Department of Chemistry, University College London, 20 Gordon Street, London WC1H 0AJ, United Kingdom, Department of Chemistry, University of Nebraska, Lincoln, Nebraska 68588, and Departamento de Quimica, ITN, Estrada Nacional 10, 2686-953, Sacavem Codex, Portugal

Received March 26, 2001

Reaction of LnI_2 (Ln = Sm, Yb) with two equivalents of $NaTp^{Me_2}$ or reduction of $Eu(Tp^{Me_2})_2OTf$ gives good yields of the highly insoluble homoleptic Ln(II) complexes, $Ln(Tp^{Me_2})_2$ (Ln = Sm (**1a**), Yb (**2a**), Eu (**3a**)). Use of the additionally 4-ethyl substituted $Tp^{Me_2,4Et}$ ligand produces the analogous, but soluble $Ln(Tp^{Me_2,4Et})_2$ (**1**−**3b**) complexes. Soluble compounds are also obtained with the Tp^{Ph} and Tp^{Tn} ligands (Tn = thienyl), $Ln(Tp^{Ph})_2$ (Ln = Sm, **1c**; Yb, **2c**) and $Ln(Tp^{Tn})_2$ (Ln = Sm, **1d**; Yb, **2d**). To provide benchmark parameters for structural comparison the series of $Sm(Tp^{Me_2})_2X$ complexes (X = F, **1e**; Cl, **1f**; Br, **1g**; I, **1h**; BPh_4, **1j**) were prepared either via oxidation of the $Sm(Tp^{Me_2})_2$ or salt metathesis from SmX_3 (X = Cl, Br, I). The solid-state structures of **1**−**3a**, **1b**, **1**−**2c** and **1e**, **1f**, **1h**, and **1j** were determined by single-crystal X-ray diffraction. The homoleptic bis-Tp complexes are all six-coordinate with trigonal antiprismatic geometries, planes of the κ^3-Tp ligands are parallel to one another. In the series of $Sm(Tp^{Me_2})_2X$ complexes the structure changes from seven-coordinate molecular compounds, with intact Sm-X bonds, for X = F, Cl, to six-coordinate ionic structures $[Sm(Tp^{Me_2})_2]X$ (X = I, BPh_4), suitable crystals of the bromide compound could not be obtained. The dependence of the structures on the size of X is understandable in terms of the interplay between the size of the cleft that the $[Sm(Tp^{Me_2})_2]^+$ fragment can make available and the donor ability of the anionic group toward the hard Sm(III) center.

Introduction

The organometallic chemistry of divalent lanthanides has witnessed an explosive growth during the past two decades.[1] The major reason for this can be traced to the remarkable reactivities of $Ln(C_5Me_5)_2$ (Ln = Sm, Eu, Yb) toward both organic and inorganic substrates, as demonstrated especially by Evans (Ln = Sm),[2] Andersen (Ln = Yb),[3] and their co-workers. Although the chemistry has been dominated by the ubiquitous cyclopentadienyl ligand system, the search for other supporting ligands has been intense[4] and in recent years bis-ligand Ln(II) complexes (Ln = Sm, Eu, Yb) with alkoxides,[5] amides,[6] phosphides,[7] chalcogenolates,[8] benzamidinates,[9] hydrocarbyls, and related Si, Ge, and Sn based ligands,[10] and nitrogen donor macrocycles[11] have been uncovered and shown to have interesting reactivities.

* To whom correspondence should be sent.
† University of Alberta.
# University College London.
‡ University of Nebraska.
§ ITN.

(1) (a) Evans, W. J. *Polyhedron* **1987**, *6*, 803. (b) Schaverien, C. J. *Adv. Organomet. Chem.* **1994**, *36*, 283. (c) Edelmann, F. T. In *Comprehensive Organometallic Chemistry II*; Abel, E. W., Stone, F. G. A., Wilkinson, G, Lappert, M. F., Eds.; Pergamon: Oxford, 1995; Vol. 4, Chapter 2.

(2) (a) Evans, W. J.; Grate, J. W.; Choi, H. W.; Bloom, I.; Hunter, W. E.; Atwood, J. L. *J. Am. Chem. Soc.* **1985**, *107*, 941. (b) Evans, W. J.; Gonzales, S. L.; Ziller, J. W. *J. Am. Chem. Soc.* **1991**, *113*, 7423 and references therein.

(3) (a) Burns, C. J.; Andersen, R. A. *J. Am. Chem. Soc.* **1987**, *109*, 5853 and references therein. (b) Shultz, M.; Burns, C. J.; Schwartz, D. J.; Andersen, R. A. *Organometallics* **2000**, *19*, 781.

(4) For a review on "Cyclopentadienyl-Free Organolanthanide Chemistry", see: Edelmann, F. T. *Angew. Chem., Int. Ed. Engl.* **1995**, *34*, 2466.

(5) (a) Hou, Z.; Fujita, A.; Yoshimura, T.; Jesaka, A.; Zhang, Y.; Yamazaki, H.; Wakatsuki, Y. *Inorg. Chem.* **1996**, *35*, 7190. (b) Evans, W. J.; Anwander, R.; Ansari, M. A.; Ziller, J. W. *Inorg. Chem.* **1995**, *34*, 5. (c) Qi, G.-Z.; Shen, Q.; Lin, Y.-H. *Acta Crystallogr., Section. C* **1994**, *50*, 1456. (d) van den Hende, J. R.; Hitchcock, P. B.; Lappert, M. F. *J. Chem. Soc., Chem. Commun.* **1994**, 1413.

(6) (a) Evans, W. J.; Drummond, D. K.; Zhang, H. M.; Atwood, J. L. *Inorg. Chem.* **1988**, *27*, 575. (b) Tilley, T. D.; Andersen, R. A.; Zalkin, A. *Inorg. Chem.* **1984**, *23*, 2271.

(7) (a) Rabe, G. W.; Guzei, I. A.; Rheingold, A. L. *Inorg. Chem.* **1997**, *36*, 4914. (b) Rabe, G. W.; Yap, G. P. A.; Rheingold, A. L. *Inorg. Chem.* **1997**, *36*, 3212. (c) Nief, F.; Ricard, L. *J. Organomet. Chem.* **1994**, *464*, 149.

(8) (a) Çetinkaya, B.; Hitchcock, P. B.; Lappert, M. F. *J. Chem. Soc., Chem. Comun.* **1992**, 932. (b) Cary, D.; Arnold, J. *Inorg. Chem.* **1994**, *33*, 1791. (c) Brewer, M.; Khasnis, D.; Buretea, M.; Berardini, M.; Emge, T. J.; Brennan, J. G. *Inorg. Chem.* **1994**, *33*, 2743. (d) Mashima, K.; Nakayama, Y.; Shibahara, T.; Fukumoto, N.; Nakamura, A. *Inorg. Chem.* **1996**, *35*, 93.

(9) Edelmann, F. T. *Coord. Chem. Rev.* **1994**, *137*, 403 and references therein.

(10) (a) Clegg, W.; Eaborn, C.; Izod, K.; O'Shaughnessy, P.; Smith, J. D. *Angew. Chem., Int. Ed. Engl.* **1997**, *36*, 2815. (b) Eaborn, C.; Hitchcock, P. B.; Izod, K.; Smith, J. D. *J. Am. Chem. Soc.* **1994**, *116*, 12071. (c) Hitchcock, P. B.; Holmes, S. A.; Lappert, M. F.; Tian, S. *J. Chem. Soc., Chem. Commun.* **1994**, 2691. (d) Bochkarev, L. N.; Makarov, V. M.; Hrzhanovskaya, Y. N. *J. Organomet. Chem.* **1994**, *467*, C3.

(11) (a) Jubb, J.; Gambarotta, S. *J. Am. Chem. Soc.* **1994**, *116*, 4477. (b) Song, J.; Gambarotta, S. *Angew. Chem., Int. Ed. Engl.* **1995**, *34*, 2141.

10.1021/ic010325w CCC: $20.00
Published on Web 08/28/2001

A versatile anionic alternative ligand system, with easily tunable steric profile, is provided by the hydrotris(pyrazolyl)-borates, $Tp^{R,R'}$. First introduced by Trofimenko,[12] the ligands have been shown to be effective complexation agents for a broad range of metal ions,[13] including f-elements.[14a−c]

Here we report full details on the synthesis and characterization of a series of bis-ligand $Ln(Tp^{R,R'})_2$ complexes (Ln = Sm, Eu, Yb) and trivalent $Sm(Tp^{Me_2})_2X$ (X = F, Cl, Br, I, BPh_4) compounds. The solid-state X-ray structures of several members have been determined and a detailed structural comparison is provided also. Some of this work has been communicated before[15] and the synthesis of $Ln(Tp^{Me_2})_2$ has been reported also by Jones and Evans.[16]

Results and Discussion

Synthesis and Characterization. $Ln(Tp^{Me_2})_2$ Complexes; Ln = Sm, Eu, Yb. Addition of THF to a 2:1 stoichiometric mixture of solid KTp^{Me_2} and LnI_2, or addition of a THF solution of KTp^{Me_2} to LnI_2 in the same solvent, resulted in an immediate color change from blue (Sm) or yellow (Yb) to purple and the precipitation of the same colored solid, mixed with KI, eq 1.

$$LnI_2 + 2KTp^{Me_2} \xrightarrow{THF} Ln(Tp^{Me_2})_2(s) + 2KI(s) \quad (1)$$
Sm (**1a**), Yb (**2a**)

The resulting products were found to be insoluble in all common aliphatic, aromatic or ether type solvents and reacted with chlorinated solvents. Although both **1a** and **2a** could be washed with oxygen-free water without significant decomposition, and were subsequently found to dissolve sparingly in carefully dried HMPA, no completely satisfactory wet route was found to separate the desired complexes from potassium iodide. Careful sublimation under high vacuum at 300 °C afforded pure $Yb(Tp^{Me_2})_2$ (**2a**). In the case of $Sm(Tp^{Me_2})_2$ (**1a**), significant decomposition occurred under these conditions. In view of these difficulties an alternative synthesis for these complexes was sought. It was discovered that use of the sodium salt, $NaTp^{Me_2}$, provides a simple, convenient synthesis, eq 2. The byproduct, NaI is fairly soluble in THF, and simple inverse filtration of the reaction mixture affords pure **1a** and **2a** in high yields.

$$LnI_2 + 2NaTp^{Me_2} \xrightarrow{THF} Ln(Tp^{Me_2})_2(s) + 2NaI(THF) \quad (2)$$
Sm (**1a**), Yb (**2a**)

It was found more convenient to prepare the europium complex, $Eu(Tp^{Me_2})_2$ (**3a**), by reduction of the trivalent triflate complex[17] with sodium mercury yielding a bright orange suspension.

$$Eu(Tp^{Me_2})_2OTf + Na/Hg \xrightarrow{THF} \underset{\textbf{3a}}{Eu(Tp^{Me_2})_2(s)} + NaOTf \quad (3)$$

Decantation of the slurry away from the amalgam followed by vacuum sublimation permitted the isolation of pure **3a** as large luminescent orange blocks. $Eu(Tp^{Me_2})_2$ is extremely thermally stable and an orange vapor can be seen in evacuated sealed tubes containing the complex at 300 °C.

All of the complexes are very sensitive to oxygen in the solid state. Their formulation is consistent with elemental analysis, mass spectra and the solid-state structures were determined by single-crystal X-ray diffraction. Infrared spectra show a single B−H stretch around 2530 cm^{-1}. The ^{13}C CPMAS NMR spectrum of **2a** shows only a single pyrazole environment and confirms the expected diamagnetism of the Yb(II) complex.

Photoelectron spectroscopy using HeIα and HeIIα radiation showed a single metal-based low energy ionization for the europium complex **3a**, at 6.46 eV, together with an envelope at higher energy associated with the pyrazolylborate ligands. The appearance of this band is consistent with it being composed of the overlapping spin−orbit components of the ^7F state. In addition the ionization energy, which is indicated by this band, is in close agreement with that of 6.3 eV observed for $[Eu(C_5Me_5)_2]$.[18] The spectra of **2a** were of poor quality and those of **1a** could not be recorded as a result of the thermal decomposition described above.

It is noteworthy that the complexes are isolated as THF free materials, contrary to the related C_5Me_5 compounds which retain varying amounts of coordinated THF.[2,3] The more congested nature of the $Ln(Tp^{Me_2})_2$ complexes is clearly indicated by this observation and presages a heightened steric control of the redox-based chemistry than that of $Ln(C_5Me_5)_2$.

$Ln(Tp^{Me_2,4Et})_2$ Complexes; Ln = Sm, Eu, Yb. In view of the extraordinary and unexpected insolubility of the $Ln(Tp^{Me_2})_2$ complexes in common solvent we felt it would be useful to attempt to increase the solubility by disrupting the packing of the complexes in the lattice and that this would be best accomplished by altering the substituents on the pyrazole groups of the ligands. Since the substituents in the 3 and 5 positions are critical in determining the steric demand of the ligand, and hence the structure of the resulting complex, substituents in the 4-position were considered. A number of workers have followed Trofimenko[19] in using either bromide or butyl substituents in this position. We were, however, concerned by the likely incompatibility of the halide with highly reducing lanthanide (II) metal centers and by the additional complexity that a butyl group might introduce into NMR spectra in the event of a mixture of products. We therefore chose to prepare 4-ethyl substituted pyrazole. 3,5-Dimethyl-4-ethylpyrazole was prepared from the corresponding 3-ethyl-pentane-2,4-dione and hydrazine hydrate and converted to the corresponding potassium tris-pyrazolyborate by standard methods (see Experimental Section).

(12) (a) Trofimenko, S. *J. Am. Chem. Soc.* **1967**, *89*, 3170. (b) Trofimenko, S. *J. Am. Chem. Soc.* **1967**, *89*, 6288.
(13) (a) Trofimenko, S. *Acc. Chem. Res.* **1971**, *4*, 17. (b) Trofimenko, S. *Chem. Rev.* **1972**, *72*, 497. (c) Shaver, A. *J. Organomet. Chem. Libr.* **1977**, *3*, 157. (d) Trofimenko, S. *Progr. Inorg. Chem.* **1986**, *34*, 115. (e) Niedenzu, K.; Trofimenko, S. *Top. Curr. Chem.* **1986**, *132*, 1. (f) Byers, P. K.; Carty, A. J.; Honeyman, R. G. *Adv. Organomet. Chem.* **1992**, *34*, 1. (g) Trofimenko, S. *Chem. Rev.* **1993**, *93*, 943. (h) Kitajima, N.; Tolman, W. B. *Prog. Inorg. Chem.* **1995**, *43*, 419. (i) Parkin, G. *Adv. Inorg. Chem.* **1995**, *42*, 291. (j) Reger, D. L. *Coord. Chem. Rev.* **1996**, *147*, 571. (k) Trofimenko, S. *Scorpionates-The Coordination Chemistry of Polypyrazolylborate Ligands*; Imperial College Press, 1999. (l) The abbreviation used for the ligands is that proposed by Trofimenko:[4g] Tp stands for tris(pyrazolyl)borate; R and R′ are substituents at the 3 and 5 positions of the pyrazolyl group, respectively and 4-substituent is denoted by the superscript 4R.
(14) (a) Santos, I.; Marques, N. *New J. Chem.* **1995**, *19*, 551. (b) Takats, J. *J. Alloys Compd.* **1997**, *249*, 52. (c) Hillier, A. C.; Liu, S. Y.; Sella, A.; Elsegood, M. R. J. *J. Alloys Compd.* **2000**, *303−304*, 83.
(15) (a) Takats, J.; Zhang, X. W.; Day, V. W.; Eberspacher, T. A. *Organometallics* **1993**, *12*, 4286. (b) Maunder, G. H.; Sella, A.; Tocher, D. A. *J. Chem. Soc. Chem. Commun.* **1994**, 885.
(16) Moss, M. A. J.; Kresinski, R. A.; Jones, C. J.; Evans, W. J. *Polyhedron*, **1993**, *12*, 1953.
(17) Liu, S. Y.; Maunder, G. H.; Sella, A.; Stevenson, M.; Tocher, D. A. *Inorg. Chem.* **1996**, *35*, 76.
(18) (a) Andersen, R. A.; Boncella, J. M.; Burns, C. J.; Green, J. C.; Hohl, D.; Rösch, N. *J. Chem. Soc., Chem. Commun.* **1986**, 405−407. (b) Green, J. C.; Hohl, D.; Rösch, N. *Organometallics* **1987**, *6*, 712−720.
(19) Trofimenko, S.; Calabrese, J. C.; Domaille, P. J.; Thompson, J. S. *Inorg. Chem.* **1989**, *28*, 1091−1101.

We were gratified to find that the reaction of $KTp^{Me_2,4Et}$ with LnI_2 (Ln = Sm, Yb) yielded deep purple THF solutions of the corresponding complexes **1b**, and **2b** from which they could be crystallized at low temperature. Similarly addition of excess sodium amalgam to a 1:2 mixture of europium triflate and $KTp^{Me_2,4Et}$ in THF gave a bright orange solution. The product, **3b** was purified by vacuum sublimation. Infrared spectra of the complexes show a single B−H stretching vibration in the region of 2525 cm^{-1} as expected. ^1H NMR spectra, consistent with the expected formulation were obtained for **1b** and **2b**, although the former was found to be somewhat shifted and broadened by the paramagnetic samarium center. ^1H NMR spectrum for **3b** could not be observed.

$Ln(Tp^{Ph})_2$ and $Ln(Tp^{Tn})_2$ Complexes; Ln = Sm, Yb; Ph = phenyl, Tn = thienyl. As in the above case addition of KTp^R to LnI_2 in THF resulted in intensely colored solutions from which dark green samarium (**1c**, **1d**) and dark red ytterbium (**2c**, **2d**) were isolated by low-temperature crystallization from toluene. As implied, and contrary to **1a** and **2a**, the complexes

$$LnI_2 + 2KTp^R \xrightarrow{THF} Ln(Tp^R)_2 + 2KI(s) \qquad (4)$$

Ln	R = Ph	Tn
Sm	**1c**	**1d**
Yb	**2c**	**2d**

are soluble in THF and toluene but only sparingly in hydrocarbon solvents. Due to their soluble nature they were characterized by ^1H NMR spectroscopy. The spectra of **1c** and **2c** exhibit one set of pyrazole resonances, five signals in a 1:1:2:2:1 ratio, indicating that the phenyl ortho and meta protons are equivalent also. This is to be contrasted to the situation with $Fe(Tp^{Ph})_2$ where fourteen proton resonances were observed.[20] It appears that in the more sterically congested iron complex the phenyl rings do not rotate freely, causing the appearance of a more complex ^1H NMR spectrum. In the present complexes phenyl ring rotation is facile since no line broadening of the signals was detected down to −100 °C. The resonances of the diamagnetic ytterbium complex are sharp and exhibit the expected coupling patterns and chemical shifts. The signals of the paramagnetic samarium complex are somewhat shifted but interestingly, with the exception of the *o*-phenyl signal, suffer minimal line broadening such that coupling remains resolved. Due to their proximity to the paramagnetic samarium center the *o*-phenyl protons show up as a broad, much shifted singlet at 15.10 ppm.

The ^1H NMR spectra of **1d** and **2d** are also simple and show that the six pyrazole rings are equivalent, this is similar to that observed for $Co(Tp^{Tn})_2$.[21] Although the steric profile of Tp^{Tn} is smaller than that of Tp^{Me_2} and Tp^{Ph}, there are no resonances for coordinated THF, indicating that the coordination environment provided by two Tp^{Tn} ligands is still too congested to allow THF to coordinate to the metal centers.

Other $Ln(Tp^R)_2$ Derivatives. The preparation of analogous homoleptic complexes of ytterbium by reaction of both thallium hydro-tris-benzotriazolylborate[22] and potassium hydro-tris-3-(2-pyridyl)pyrazolylborate[23] gave extremely air-sensitive deep purple solutions from which solids were obtained. In all cases appropriate B−H stretching vibrations were observed in the infrared spectra and a readable ^1H NMR spectrum was obtained, but no tractable crystalline or even analytically pure solid materials could be obtained.

Reactivity of $Ln(Tp^{R,R'})_2$ Complexes: Preparation of $Sm(Tp^{Me_2})_2X$ (X = F, Cl, Br, I, BPh_4)

In view of the spectacular reactivity of decamethylsamarocene with unsaturated organic molecules[2] it was of obvious interest to compare the reactivity of the pyrazolylborate systems with the cyclopentadienyls. Although we have recently shown that $Sm(Tp^{Me_2})_2$ has very interesting one-electron reduction chemistry[14b,15] and is able to provide a particularly well suited pocket to stabilize reactive radical species, including the superoxide anion,[24] the chemistry is more selective than that of $Sm(C_5Me_5)_2$. Thus when **1a** and **2a** are exposed to carbon monoxide, isonitriles, and a variety of alkynes including phenylacetylene, diphenylacetylene and butyne, no reaction is observed and the starting material is recovered unchanged. In fact, we found that the soluble $Sm(Tp^{Tn})_2$ is unreactive toward azobenzene whereas the insoluble $Sm(Tp^{Me_2})_2$ readily gives a soluble derivative.[15a] We attribute this behavior to the absence of any particularly facile oxidative reaction pathway available and the steric congestion at the metal center.

Despite the lack of general redox reactivity the compounds are readily oxidized to the corresponding Ln(III) derivatives. The series of $Sm(Tp^{Me_2})_2X$ complexes (X = halide and BPh_4) provide important comparison to the related "$Ln(C_5Me_5)_2X$" compounds,[25] materials that were largely responsible for the phenomenal growth and spectacular achievements in organo f-element chemistry.

The failure of complexes to react with a range of alkynes led us to investigate the reaction of $Sm(Tp^{Me_2})_2$ (**1a**) with hexafluorobutyne (HFB, $CF_3C{\equiv}CCF_3$). The reaction proceeds by decolorization of **1a**, the only product obtained from the reaction was the fluoride, $Sm(Tp^{Me_2})_2F$ (**1e**), resulting from attack at the C−F bond rather than of the alkyne itself. Activation of C−F bonds of perfluoro olefins by $Ln(C_5Me_5)_2L$ (Ln = Sm, Eu, Yb; L = Et_2O, THF),[26a] perfluorobenzene by $Yb(C_5Me_5)_2$[26b] and saturated perfluorocarbons by $Yb(C_5H_5)_2(DME)$[26c,d] (DME = dimethoxy ethane) have been reported by Watson, Andersen and Deacon, respectively. However, a more rational synthesis is provided by deliberate oxidation of **1a** with PbF_2, which gives colorless **1e** in good yield,[27] eq 5.

$$2Sm(Tp^{Me_2})_2 + PbF_2 \rightarrow 2Sm(Tp^{Me_2})_2F + Pb(s) \qquad (5)$$
$$\textbf{1e}\ (82\%)$$

Compounds **1a**−**3a** and **1b**−**3b** react with chloro and bromocarbon compounds. The more insoluble Tp^{Me_2} complexes often survive for several hours but ultimately all materials are

(20) Eichhorn, D. M.; Armstrong, W. H. *Inorg. Chem.* **1990**, *29*, 3607.
(21) Calabrese, J. C.; Domaille, P. J.; Trofimenko, S.; Long, G. J. *Inorg. Chem.* **1991**, *30*, 2795.
(22) Lalor, F. S.; Miller, S. M.; Garvey, N. *Polyhedron* **1990**, *9*, 63.
(23) (a) Jones, P. L.; Amoroso, A. J.; Jeffrey, J. C.; McCleverty, J. A.; Psillakis, E.; Rees, L. H.; Ward, M. D. *Inorg. Chem.* **1997**, *36*, 10. (b) Trofimenko, S. Personal communication.
(24) Zhang, X. W.; Loppnow, G. R.; McDonald, R.; Takats, J. *J. Am. Chem. Soc.* **1995**, *117*, 7628.
(25) Schumann, H.; Meese-Marktscheffel, J. A.; Esser, L. *Chem. Rev.* **1995**, *95*, 865 and references therein.
(26) (a) Watson, P. L.; Tulip, T. H.; Williams, I. *Organometallics* **1990**, *9*, 1999. (b) Burns, C. J.; Andersen, R. A. *J. Chem. Soc., Chem. Commun.* **1989**, 136. (c) Deacon, G. B.; Harris, S.; Meyer, G.; Stellfeldt, D.; Wilkinson, D. L.; Zelesny, G. *J. Organomet. Chem.* **1998**, *552*, 165. (d) Deacon, G. B.; Meyer, G.; Stellfeldt, D. *Eur. J. Inorg. Chem.* **2000**, 1061.
(27) For the application of oxidation strategy to the synthesis of $LnCp_2'XL$ from Ln(II) precursors see: (a) Deacon, G. B.; Harris, S. C.; Meyer, G.; Stellfeldt, D.; Wilkinson, D. L.; Zelesny, G. *J. Organomet. Chem.* **1996**, *525*, 247 and ref 26 (c) for Ln = Yb. See: (b) Schumann, H.; Keitsch, M. R.; Winterfeld, J.; Demtschuk, J. *J. Organomet. Chem.* **1996**, *525*, 279 for Ln = Sm.

decolorized and the corresponding chlorides and bromides are obtained. However, salt metathesis provides a more rational and higher yield route to $Sm(Tp^{Me_2})_2Cl$ (**1f**) and $Sm(Tp^{Me_2})_2Br$ (**1g**). Thus, stirring SmX_3 (X = Cl or Br) with KTp^{Me_2} in THF results in the formation of a white precipitate (KCl, KBr) and isolation of toluene soluble **1f** and **1g**, eq 6.

$$SmX_3 + 2KTp^{Me_2} \xrightarrow{THF} Sm(Tp^{Me_2})_2X + 2KX(s) \quad (6)$$
$$X = \text{Cl, } \mathbf{1f}\ (85\%)$$
$$\text{Br, } \mathbf{1g}\ (15\%)$$

The synthesis of **1g** proved to be somewhat unreliable and correct elemental analyses were not obtained reproducibly and in several reactions significant amounts of unidentified side-products could be seen by ^1H NMR spectroscopy. Thus, **1g** is significantly less stable than either the chloride or the iodide (vide infra). Attempts to recrystallize the complex from toluene often gave less pure material than the crude reaction product and we were unable, despite repeated attempts, to isolate a crystalline sample.

The toluene solubility of **1e**−**1g** suggests the presence of molecular compounds, i.e., preservation of the Ln−X bond and seven-coordinate molecular structure. That this is the case will be corroborated by the X-ray structures of the complexes **1e** and **1f**. The simple ^1H NMR spectrum, one set Tp^{Me_2} resonances, indicates rapid fluxionality in solution.

Contrary to the above, addition of I_2 to a slurry of $Sm(Tp^{Me_2})_2$ in THF or $NaTp^{Me_2}$ to a THF solution of $SmI_3(THF)_3$ produced $Sm(Tp^{Me_2})_2I$ (**1h**) as a white, THF insoluble precipitate, eq 7. The insolubility of **1h** indicates that it is more properly formulated as the iodide salt of $[Sm(Tp^{Me_2})_2]^+$.

$$Sm(Tp^{Me_2})_2(s) + 1/2I_2 \xrightarrow{THF}$$
$$[Sm(Tp^{Me_2})_2]I(s) \xleftarrow[-2NaI]{THF} SmI_3(THF)_3 + 2NaTp^{Me_2} \quad (7)$$
$$\mathbf{1h}\ (67-75\%)$$

Addition of further iodine to **1a** results in the formation of the corresponding triiodide salt $[Sm(Tp^{Me_2})_2]I_3$, **1i**, which is likewise insoluble in toluene as expected for such a salt. The corresponding BPh_4^- salt was prepared by $TlBPh_4$ oxidation of **1a**, eq 8. This salt is solutle in THF.

$$Sm(Tp^{Me_2})_2(s) + TlBPh_4 \xrightarrow{THF} [Sm(Tp^{Me_2})_2]BPh_4 + Tl(s) \quad (8)$$
$$\mathbf{1j}\ (50\%)$$

Noteworthy features of complexes **1h**−**1j**, which again reflect the steric size of the Tp^{Me_2} ligands, are the lack of coordinated THF and the inability of $Sm(Tp^{Me_2})_2^+$ fragment to retain the Sm−I bond. The corresponding $Sm(C_5Me_5)_2I$ is molecular and indeed has sufficient room to accommodate a THF ligand.[28]

Crystallographic Studies

Solid State Structures of the $Ln(Tp^{Me_2})_2$, $Sm(Tp^{Me_2,4Et})_2$ and $Ln(Tp^{Ph})_2$ Complexes. Complexes **1a**, **2a**, and **3a** are isomorphous crystallizing in the trigonal space group $R\bar{3}$ (No. 148). The complexes therefore possess crystallographic S_6 symmetry consistent with the observation of a single pyrazole environment in the ^{13}C CPMAS NMR spectrum of **2a**. The

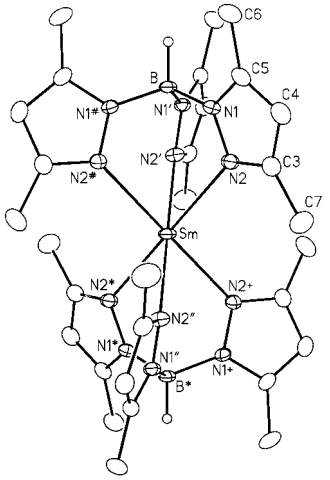

Figure 1. Molecular structure of $Sm(Tp^{Me_2})_2$, **1a**. The atoms are drawn with 20% probability ellipsoids. Hydrogen atoms have been omitted for clarity. The samarium atom is located at the unit cell origin, which is a $\bar{3}$ center of symmetry, thus primed atoms are related to unprimed ones via the symmetry operation (z, x, y), double-primed atoms by ($\bar{z}$, $\bar{x}$, $\bar{y}$), starred atoms by ($\bar{x}$, $\bar{y}$, $\bar{z}$), atoms marked with an octothorpe (#) by (y, z, x), and atoms marked with a plus (+) by ($\bar{y}$, $\bar{z}$, $\bar{x}$).

metal atom lies at the origin of the unit cell, the boron atoms and the corresponding hydrogen atoms lying on the C_3-S_6 axis. The symmetrical, trigonal antiprismatic structure is in stark contrast to the corresponding unsolvated metallocene "sandwich" complexes of europium and samarium[29] in which the Cp-centroid to metal vectors meet at an angle of 140.1° (Sm) and 144° (Eu) in the solid state. As a representative, the structure of $Sm(Tp^{Me_2})_2$ (**1a**) is shown in Figure 1. The tridentate Tp^{Me_2} groups lie in a staggered arrangement around the metal center with the methyl groups sitting in the cleft between the pyrazolyl groups of the other ligand. This is again in contrast to the decamethylmetallocenes and also to those complexes of the less substituted Tp ligand[30] since the metal is well protected from incoming ligands and the complexes are only obtained in base-free form. Relevant metrical parameters on these and related $Ln(Tp')_2$ complexes are collected in Table 1.

The angles subtended by the pyrazolyl groups at boron are essentially tetrahedral. The large size of the metal atom in all three structures is therefore accommodated by a slight twisting of the pyrazolyl groups around the B−N bonds (13°) and the attendant B−N−N−Ln torsion angles (21°). The metal nitrogen distances can thus be seen to decrease in step with the increase in the atomic number of the metal: **1a** 2.616(2) Å, **3a** 2.597(2) Å, **2a** 2.482(3) Å. Hence these three structures together with the barium[31] and lead[32] complexes offer an unusual situation in which the lanthanide contraction may be observed directly, unobscured by changes in structure and coordination number.

One of the most intriguing features of these complexes is their extreme insolubility. The crystal structures however reveal no close intermolecular contacts that might contribute to this

(28) (a) Evans, W. J.; Grate, J. W.; Levan, K. R.; Bloom, I.; Peterson, T. T.; Doedens, R. J.; Zhang, H.; Atwood, J. L. *Inorg. Chem.* **1986**, *25*, 3614. (b) Evans, W. J.; Drummond, D. K.; Hughes, L. A.; Zhang, H.; Atwood, J. L. *Polyhedron* **1988**, *7*, 1693.

(29) Evans, W. J.; Hughes, L. A.; Hanusa, T. P. *Organometallics* **1986**, *5*, 1285.

(30) Domingos, A.; Marçalo, J.; Marques, N.; Pires de Matos, A.; Galvão, A.; Isolani, P. C.; Vicentini, G.; Zinner, K. *Polyhedron* **1995**, *14*, 3067.

(31) (a) Dutremez, S. G.; Leslie, D. B.; Streib, W. E.; Chisholm, M. H.; Caulton, K. G. *J. Organomet. Chem.* **1993**, *462*, C1. (b) Belderraín, T. R.; Contreras, L.; Paneque, M.; Carmona, E.; Monge, A.; Ruiz, C. *J. Organomet. Chem.* **1994**, *474*, C5. (c) Belderraín, T. R.; Contreras, L.; Paneque, M.; Carmona, E.; Monge, A.; Ruiz, C. *Polyhedron* **1996**, *15*, 3453.

(32) Reger, D. L.; Huff, M. F.; Rheingold, A. L.; Haggerty, B. S. *J. Am. Chem. Soc.* **1992**, *114*, 579.

Table 1. Average Interatomic Distances (Å) and Angles (deg) and Ranges in the Individual Metrical Parameters for $Sm(Tp^{Me_2})_2$ (**1a**), $Yb(Tp^{Me_2})_2$ (**2a**), $Eu(Tp^{Me_2})_2$ (**3a**), $Sm(Tp^{Me_2,4Et})_2$ (**1b**), $Sm(Tp^{Ph})_2$ (**1c**), and $Yb(Tp^{Ph})_2$ (**2c**)

	1a	2a[a]	3a	1b	1c	2c
$Ln-N(pz)_{av}$	2.616(2)	2.482(3) 2.480(4)	2.597(2)	2.615(4)	2.677(20)	2.550(14)
$Ln-N(pz)_{range}$				2.609(3)−2.623(3)	2.648(2)−2.714(2)	2.536(2)−2.577(2)
Ln···B	3.627(3)	3.474(4)	3.590(3)	3.687(2)	3.605(5)	3.435(4)
$N-Ln-N(intra)_{av}$	75.47(7)	79.5(1)	76.18(6)	73.7(5)	76.5(9)	80.9(14)
$N-Ln-N(intra)_{range}$				72.8(1)−74.6(1)	75.27(7)−78.26(8)	78.50(8)−83.43(8)
$N-Ln-N(inter)_{av}$	104.53(7)	100.5(1)	103.82(6)	106.3(5)	103.5(9)	99.1(14)
$N-Ln-N(inter)_{range}$				105.4(1)−107.2(1)	101.74(8)−104.73(7)	96.57(8)−101.50(8)
$N-B-N_{av}$	110.9(2)	110.7(2)	111.1(1)	111.1(3)	112.0(11)	111.8(9)
$N-B-N_{range}$				110.7(3)−111.6(3)	110.9(3)−114.3(3)	110.2(3)−113.4(3)
			Torsion Angles			
$Ln-N-N-B_{av}$	21.1(3)	20.5(4)	20.7(2)	5.6(18)	9.5(13)	9.5(20)
$Ln-N-N-B_{range}$				2.2(4)−8.0(4)	7.6(4)−11.9(3)	5.6(4)−12.0(3)

[a] Results of two independent determinations, one at UA and one at UCL.

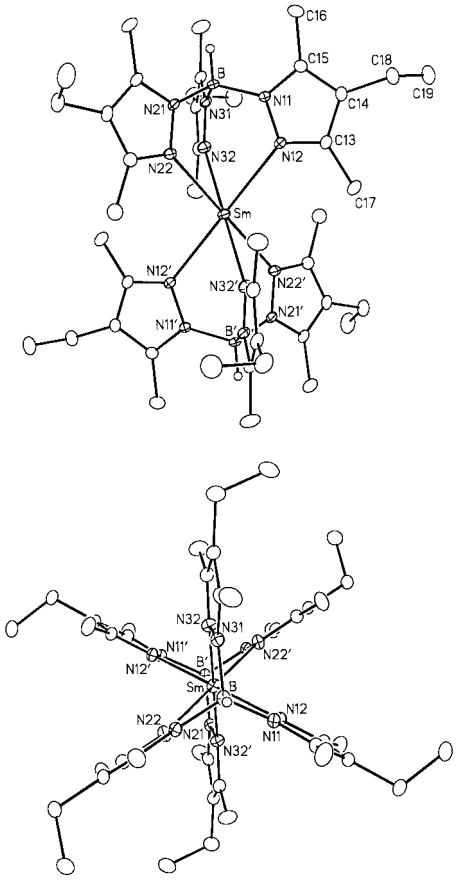

Figure 2. (a) Molecular structure of $Sm(Tp^{Me_2,4Et})_2$, **1b**. The atoms are drawn with 20% probability ellipsoids. Hydrogen atoms have been omitted for clarity. Primed atoms are related to unprimed ones via the crystallographic inversion center (0, 0, 0) upon which the Sm atom is located. (b) Alternate view of the molecule approximately along the B···Sm···*B* axis, illustrating the dispositions of the ethyl groups.

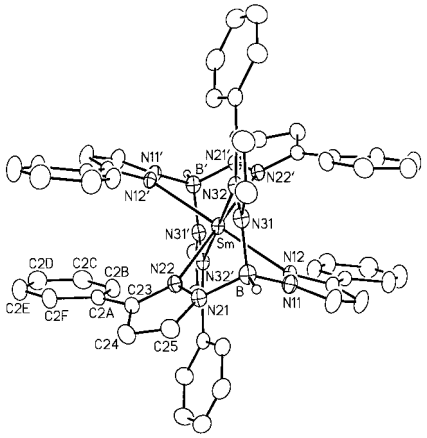

Figure 3. Molecular structure of $Sm(Tp^{Ph})_2$, **1c**. The atoms are drawn with 20% probability ellipsoids. Hydrogen atoms have been omitted for clarity. Primed atoms are related to unprimed ones via the crystallographic inversion center (0, 0, 0) upon which is located the samarium atom.

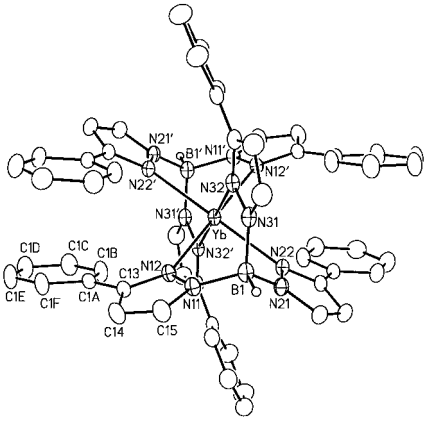

Figure 4. Molecular structure of $Yb(Tp^{Ph})_2$, **2c**. The atoms are drawn with 20% probability ellipsoids. Hydrogen atoms have been omitted for clarity. Primed atoms are related to unprimed ones via the crystallographic inversion center (0, 0, 0) upon which is located the ytterbium atom.

behavior. The insolubility must therefore be attributed to the efficiency of the packing of these nearly spherical complexes in the solid state. Indeed, this is reflected in the hexagonal close packed lattice adopted, which we presume leads to a particularly favorable lattice energy. At the same time no particular charge asymmetries are present in these very compact structures and this ensures that interactions with polar solvents, for example, will be fairly insignificant and hence solubility will be low.

The structure of **1b** is shown in Figure 2 and is largely similar to that observed for the corresponding insoluble analogues and shows no evidence for intermolecular contacts. The Sm−N distance, 2.615(4) Å is identical to that in **1a** confirming that the presence of the ethyl group makes little or no difference to the binding properties of the ligand. Other bond distances and angles are also very similar those of **1a.** The ethyl groups are rotated approximately perpendicular to the B−Sm−B axis with two oriented toward each other and one away.

The structures of $Ln(Tp^{Ph})_2$ (Ln = Sm, **1c**; Yb, **2c**) are shown in Figures 3 and 4, respectively. As with the other bis-Tp′ lanthanide complexes the coordination geometry is trigonal

antiprismatic and, in the present cases, possesses C_i crystallographic symmetry. The trigonal distortion of the coordination geometry is evidenced by the less than ideal octahedral value of 90° for the intraligand N−Ln−N bond angles and the larger than 90° interligand N−Ln−N angles. The average Sm−N (2.677(20) Å) and Yb−N (2.550(14) Å) distances are some 0.06 Å longer than those observed in **1a** and **2a**, respectively, and reflect the bulkier nature of the Tp^{Ph} ligand. The contraction in Ln-N distance on going from **1c** to **2c** (0.13 Å) is almost identical to that observed in the **1a** to **2a** transition (0.14 Å).

Interestingly the Ln···B nonbonded distances in **1a**/**1c** and **2a**/**2c** are almost the same. Consequently the larger Ln−N distances with the Tp^{Ph} ligand are not accommodated by pulling the Tp^{Ph} ligand away from the Ln(II) center along the Ln···*B* axis but by a slight spreading the pyrazolyl rings further apart. This is seen by the marginally larger average intraligand N−B−N angles in **1c**/**2c** (112(1)°) compared to **1a**/**2a** (110.8(2)°). The average intraligand N−Ln−N angles in **2a** (79.5(1)°) and **2c** (80.9(14)°) are larger than those in **1a** (75.5(1)°) and **1c** (76.5(9)°). This is as expected for the larger size of Sm(II) compared to Yb(II). The trigonal Tp ligand provides a pocket-like environment to the metal. Therefore, the smaller the metal and the shorter the M−N distance, the deeper the pocket and the intraligand N−M−N angle increases. Similar changes in M−N distance and N−M−N angle are noted in the following series of main group $M(Tp^{Me_2})_2$ complexes (M = Ba,[31] Sr,[33] Pb,[32] Ca,[33] Mg[34]). As the size of the metal decreases (Ba > Sr ≈ Pb > Ca > Mg) the intraligand N−M−N angle increases Ba (71.3(1)°) < Sr (74.4(12)°) < Pb (75.2(11)°) < Ca (80.0(1)°) < Mg (86.1(1)°). Indeed, as point out by Carmona,[31c] the intraligand N−M−N angles in the Sm (**1a**)/Sr and Yb (**2a**)/Ca complexes are comparable as expected from the essentially identical effective ionic radii.[35]

The B−N−N−Ln torsional angles in the Tp^{Ph} complexes, **1c** and **2c**, are much smaller (average 9.5(15)°) than those found in the Tp^{Me_2} complexes, **1a** and **2a** (average 20.7(4)°), and most probably reflect the presence of the bulkier phenyl substituent at the 3-position of the pyrazolyl moiety.

The phenyl rings in **1c** and **2c** are not coplanar with the pyrazolyl ligands. The dihedral angles are in the range 11−31° for **1c** and 21−28° for **2c** and are similar to those observed in $Fe(Tp^{Ph})_2$ (21−31°).[20]

Solid State Structures of the $Sm(Tp^{Me_2})_2X$ Complexes. The results of the X-ray diffraction studies on complexes **1e** and **1f** confirmed their formulation as $[Sm(Tp^{Me_2})_2X]$, perspective views of the molecular structures are shown in Figures 5 and 6, respectively. The central Sm(III) ion is therefore seven-coordinate, with two tridentate Tp^{Me_2} ligands and the bound halide. The pyrazolylborate ligands are as usual, staggered with respect to each other, and are bent back away from the halide anion. The B−Sm−B angle is 144.4° and 145.7°, respectively, closely comparable to that in $[Nd(Tp^{Me_2})_2OTf]$.[17] However the nature of the ligand distribution is different than in the related "bent metallocene" type lanthanide structures, $(C_5Me_5)_2Ln$ and $(C_5Me_5)_2Ln(X)(Y)$. In the latter complexes simple bending of the two C_5Me_5 ligands in the vertical plane of the putative symmetrical sandwich structure gives the "bent metallocene" geometry. Slippage and twisting of the Tp^{Me_2} ligands occur in the transformation from **1a** to **1e** and **1f**, hence the molecular symmetry is not C_s, with the halide ligand in this plane, but at most C_2; the approximate C_2 symmetry axis is formed by X, Sm and the midpoint of N(32) and N(62). The coordination geometry is best described as distorted pentagonal bipyramidal with N(12) and N(42) occupying apical sites. The Sm−N distances are somewhat shorter for these apical atoms (ave. 2.49 Å) than for those in the equatorial sites (ave. 2.63 Å), not surprising in view of the more congested nature of the latter environments. The pyrazolylborate ligand itself is unremarkable, the angles at boron being tetrahedral and average B−N−N angle being 120°. As commonly observed, significant distortions of the pyrazolylborates are apparent from the B−N−N−Sm torsion angles. The distortion roughly follows the approximate C_2 symmetric structure of the complexes which relate pyrazolyl rings 1 and 4, 2 and 5, and 3 and 6. The values of the torsion angles in **1e** and **1f** are 20.7°/26.2°, 26.8°/26.2°, and 4.0°/9.6°, and 33.1°/20.9°; 22.3°/22.9°, 2.0°/2.4°, respectively.

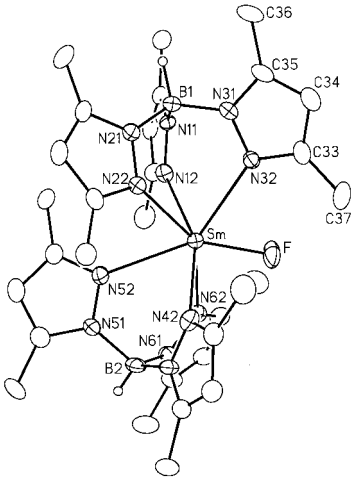

Figure 5. Molecular structure of $Sm(Tp^{Me_2})_2F$, **1e**. The atoms are drawn with 20% probability ellipsoids. Hydrogen atoms have been omitted for clarity.

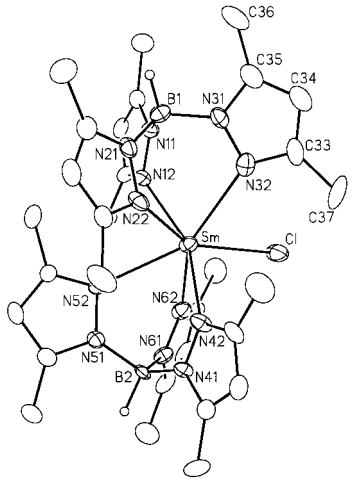

Figure 6. Molecular structure of $Sm(Tp^{Me_2})_2Cl$, **1f**. The atoms are drawn with 20% probability ellipsoids. Hydrogen atoms have been omitted for clarity.

The average Sm−N distances, **1e** (2.58 Å) and **1f** (2.56 Å), are very similar to those observed in $[Sm(Tp^{Me_2})_2EAr]$ (E = O, S, Se, Te) (2.57, 2.53, 2.54, 2.54 Å, respectively).[36] The Sm−F and Sm−Cl distances are 2.090(7) and 2.637(3) Å, respectively. The terminal Sm−Cl distance can be directly compared to that

(33) Sohrin, Y.; Matsui, M.; Hata, Y.; Hasegawa, H.; Kokusen, H. *Inorg. Chem.* **1994**, *33*, 4376.
(34) Han, R.; Parkin, G. *J. Organomet. Chem.* **1990**, *353*, C43.
(35) Shannon, R. D. *Acta Crystallogr. A* **1976**, *32*, 751.
(36) Hillier, A. C.; Liu, S. Y.; Sella, A.; Elsegood, M. R. J. *Inorg. Chem.* **2000**, *35*, 2635.

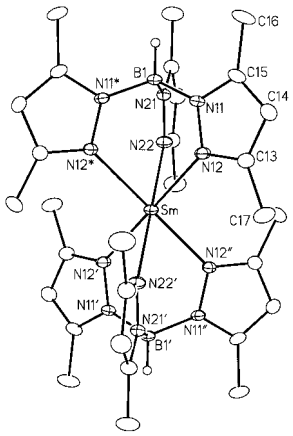

Figure 7. Perspective view of $[Sm(Tp^{Me_2})_2]^+$ ion in $Sm(Tp^{Me_2})_2I$, **1h**. The atoms are drawn with 20% probability ellipsoids. Hydrogen atoms have been omitted for clarity. Primed atoms are related to unprimed ones via the crystallographic inversion center ($^1/_2$, 0, $^1/_2$) upon which the samarium atom is located; double-primed atoms are related to unprimed ones via the crystallographic 2-fold axis ($^1/_2$, *y*, $^1/_2$); starred atoms are related to unprimed ones via the crystallographic mirror plane (*x*, 0, *z*).

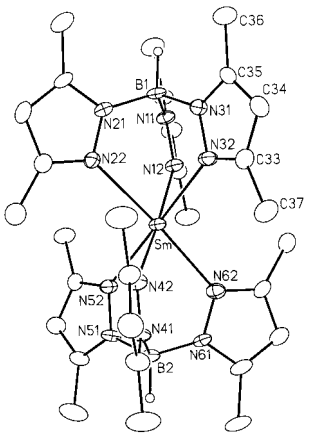

Figure 8. Perspective view of $[Sm(Tp^{Me_2})_2]^+$ ion in $Sm(Tp^{Me_2})_2BPh_4$, **1j**. The atoms are drawn with 20% probability ellipsoids. Hydrogen atoms have been omitted for clarity.

in $(C_5Me_5)_2SmCl(THF)$ (average of 2.73(1) Å)[27a] and is very similar to it once allowance is made for the 0.06 Å larger ionic radius of the eight-coordinate Sm(III)[35] in the latter complex. There are no suitable Sm complexes with terminal fluorides for direct comparison. As expected the terminal Sm−F distance in **1e** is significantly shorter than Sm−F−Sm bridging distances found in trimeric $[(C_5H_4{}^tBu)_2SmF]_3$ (average 2.24(1) Å)[27b] and dimeric $[\{(Me_3Si)_2C_5H_3\}_2SmF]_2$ (average, 2.30(1) Å).[37] The most appropriate comparison is with $(C_5Me_5)_2YbF(L)$[26a] in which the terminal Yb−F distances are 2.026(2) Å (L = THF) and 2.015(4) Å (L = Et_2O) and seem to be only slightly shorter than in **1e** once the difference of 0.035 Å is taken into consideration between the smaller eight-coordinate Yb(III) in the latter and seven-coordinate Sm(III) in **1e**. The main difference between $Sm(Tp^{Me_2})_2X$ and $Ln(C_5Me_2)_2X(L)$ is the presence of a coordinated Lewis base and the increase in coordination number from seven to eight. This is easily understood based on the sterically much more demanding nature of the Tp^{Me_2} ligand compared to C_5Me_5. Indeed the sum of the steric coordination numbers of the ligands[38] in **1e**/**1f** is almost a full unit larger than in the analogous pentamethylcyclopentadienyl derivatives, clearly leaving no room for coordination of a Lewis base. Conversely the great similarity between the structures of **1e** and **1f** and the normal Sm−X bond distances indicate that the pocket created by movement of the two Tp^{Me_2} ligands are of the right size to accommodate both halide ligands without undue weakening of the respective Sm−X bonds.

Again confirming the expectations based on solubility behavior the structures of **1h** and **1j** consist of well-separated discrete cations and anions. Ortep views of the cations are shown in Figures 7 and 8. In **1h** the cation lies on a site of 2/*m* symmetry, with a mirror plane passing through two of the pyrazolyl rings (N2), **1j** has no crystallographically imposed symmetry. The structures strongly resemble the analogous divalent $Ln(Tp')_2$ complexes. The samarium center is six-coordinate and displays a trigonal antiprismatic coordination geometry with the planes defined by the nitrogen donor atoms of each Tp^{Me_2} ligand being parallel, this is imposed by symmetry in the case of **1h**. As before, the trigonal distortion is imposed by the relatively rigid tripodal Tp^{Me_2} ligand resulting in less than 90° intraligand N−Sm−N angles (av 78.0(11)°) and larger than 90° interligand N−Sm−N angles (av 102.5(9)°). The N−B−N angles average 110.3(5)°, consistent with essentially tetrahedral geometry. As expected from the smaller sizes of the Sm(III) center, the average Sm−N distances in **1h** (2.444(12) Å) and **1j** (2.443(7) Å) are considerably shorter than in **1a** (2.616(2) Å), but very similar to that in $[Sm(Tp^{Me_2})_2](TePh)_3$ (2.45(5) Å).[39] Although there is no tabulated value for the ionic radius of six-coordinate Sm(III),[35] the difference of 0.17 Å between the average Sm−N distances of **1a** and **1h**/**1j** is only slightly smaller than the estimated difference of 0.21 Å, based either on extrapolated ionic radius of six-coordinate Sm(III) or differences between seven- or eight-coordinated Sm(II) and Sm(III).[35] Indeed, the decrease in the average Sm−N separation closely matches that observed between $Yb(Tp^{Me_2})_2$ (**2a**) and $[Yb(Tp^{Me_2})_2]^+$ (0.16 Å).[15b] Also, as observed in these latter two complexes, the oxidation of the samarium center is accompanied by a slippage of the ligand along the Sm−B vector. And again, the decrease in Sm−B distance from 3.627(3) Å in **1a** to 3.50/3.51 in **1h**/**1j** (0.12 Å) is the same as between the analogous ytterbium complex (3.468(4) and 3.348(4) Å, for a difference of 0.12 Å). Interestingly, the smaller Sm(III) ion is able to better accommodate the two Tp^{Me_2} ligands as evidenced by the reduction of the B−N−N−Sm torsion angles from 21.1(3)° in **1a** to an average of 6.0° in **1h**/**1j**.

Conclusions

A series of $Ln(Tp^{R,R'})_2$ complexes has been prepared. Reflecting the sterically more demanding nature of the $Tp^{R,R'}$ ligands compared with the ubiquitous Cp systems, the complexes are isolated free of donor solvent. They display classical trigonal antiprismatic structures with the nitrogen donors of the $Tp^{R,R'}$ ligands defining parallel planes. The reactivity of these complexes is significantly suppressed compared to that of the corresponding metallocenes. Thus, although the strongly reducing $[Sm(Tp^{Me_2})_2]$ complex can be oxidized with suitable reagents it does not react with common organic substrates such as CO, isonitriles, unactivated olefins, etc. Halide complexes can be prepared either by redox methods or in suitable cases by metathesis. The nature of the halide complexes depends on the size of the halide anion. With F^- and Cl^-, seven-coordinate molecular complexes are formed with retention of the Sm−X

(37) Xie, Z.; Liu, Z.; Mak, T. C. W. *J. Organomet. Chem.* **1997**, *539*, 127.
(38) Marçalo, J.; Pires de Matos, A. *Polyhedron* **1989**, *8*, 2431.
(39) Hillier, A. C.; Liu, S.-Y.; Sella, A.; Elsegood, M. R. J. *Angew Chem., Int. Ed.* **1999**, *38*, 2745.

bond. By contrast, the larger iodide anion adopts an ionic structure, $[Sm(Tp^{Me_2})_2]I$, in which the samarium center is six-coordinate. Although no suitable crystals of the bromide could be obtained for X-ray structural investigation to verify its structure, the solubility of the complex in chloroform or toluene strongly suggests a molecular compound. The marked instability of this compound, when compared with the other halides, points toward considerable steric strain in such a seven-coordinate structure and is an indication that it is with Br^- that the limit between molecular and ionic structures is reached. Thus, under appropriate conditions, the pocket afforded by the$[Sm(Tp^{Me_2})_2]^+$ fragment is effective for the binding of anionic ligands. In addition to the halides, complexes containing reactive radical anions and unusual functionalities have since been isolated. Work to develop this chemistry and to broaden the use of Tp ligands as ancillaries for the lanthanides continues.

Experimental Section

General Procedures. The divalent lanthanide complexes are extremely air sensitive, therefore all preparations and subsequent manipulations were carried out using standard Schlenk line and drybox techniques in an atmosphere of dinitrogen.[40] Oxygen-free nitrogen was further purified by passage over columns containing BASF Cu based catalyst (Re-11) at 100 °C and Aquasorb (Mallinckrodt, P_2O_5 on an inert support) or 3 Å molecular sieves and MnO.[41] Glassware was routinely dried at 250 °C and cooled by a nitrogen atmosphere prior to use. All solvents were predried over 5 Å molecular sieves or sodium wire (UCL). Hexane and pentane were washed with sulfuric acid and dried over $MgSO_4$ prior to distillation (U of A). The solvents were distilled from appropriate drying agents before use; Na (toluene, hexane, HMPA), K (benzene), K/benzophenone ketyl (THF), Na/K alloy (petroleum ether bp 40−60 °C, pentane, diethyl ether), $CaH_2(CH_2Cl_2)$. The deuterated solvents for NMR (THF-d_8, benzene-d_6 and toluene-d_8) were vacuum distilled from Na/K alloy (1:3), $CDCl_3$ from P_2O_5. All solvents were degassed prior to use.

THF solutions of SmI_2,[42a] or solid $SmI_2(THF)_3$[42b] and $YbI_2(THF)_{3.5}$[26a] were prepared from the metals by published procedures. The THF content was established by elemental analysis and the lanthanide metals were purchased from CERAC Inc. $SmI_3(THF)_3$ was obtained by reacting $SmI_2(THF)_3$ with 0.5 equivalents of I_2 (sublimed prior to use) in THF. Lanthanide triflates were prepared from lanthanide oxides (99.9% Berkshire Ores) and aqueous trifluoromethanesulfonic acid (Aldrich).[43] Thallium ethoxide was prepared from thallium metal[44] and $TlBPh_4$ by reacting Tl_2SO_4 with $NaBPh_4$ in aqueous solution. The ligands, potassium and sodium hydrotris(3,5-dimethylpyrazolyl)borate (Na/KTp^{Me_2}),[12b] potassium hydrotris(3-phenylpyrazolyl)borate (KTp^{Ph})[45] and potassium hydrotris((3−2′-thenyl)pyrazolyl)borate (KTp^{Tn}),[21] were prepared by literature methods.

Infrared (IR) spectra were recorded as KBr pellets on a Nicolet 205 or BOMEM MB-100 FTIR spectrometer. NMR samples were prepared in the drybox and sealed under vacuum. ^1H NMR spectra in solution were recorded on Varian XL-200 and VXR-400 or Bruker AM-400 FT spectrometers at 200 and 400 MHz, respectively. ^{11}B NMR spectra were recorded on the Bruker AM-400 instrument at 128 MHz. Spectra were calibrated using residual proton resonances (THF-d_8, 1.72 ppm; toluene-d_8, 2.09 ppm; benzene-d_6, 7.15 ppm; $CDCl_3$-d_1, 7.24 ppm) and are reported relative to tetramethylsilane (TMS). ^{11}B chemical shifts are reported relative to external $F_3B{\cdot}OEt_2$. Solid-state NMR spectra were recorded on a Bruker MSL-300 FT spectrometer at 75.468 MHz. Mass spectra were obtained on an AEI MS-12 spectrometer using electron ionization techniques. Elemental analyses were determined by Mr. Alan Stones of the UCL Analytical Services or the Microanalytical Laboratory, Department of Chemistry, University of Alberta.

Synthetic Procedures. $Sm(Tp^{Me_2})_2$ (1a). A solution of $NaTp^{Me_2}$ (640 mg, 2.0 mmol) in ca. 20 mL of THF was added dropwise to 10.0 mL of 0.1 M SmI_2 in THF. A dark purple precipitate formed immediately. The mixture was stirred overnight at room temperature and then filtered. The precipitate was washed twice with 10 mL THF and dried under dynamic vacuum. The product was isolated as a purple solid (670 mg, 90%). Single crystals of **1a** suitable for X-ray diffraction were grown by slow diffusion of a THF solution of $NaTp^{Me_2}$ into a THF solution of SmI_2 over several weeks. IR (KBr, cm^{-1}) ν_{B-H} 2540; MS (EI, 70 eV, 200 °C) *m*/*z* 746 (M^+). Anal. Calcd for $C_{30}H_{44}N_{12}B_2Sm$: C, 48.34; H, 5.91, N, 22.56. Found: C, 48.60; H, 5.98; N, 21.87.

$Yb(Tp^{Me_2})_2$ (2a). YbI_2 (2.0 g, 4.69 mmol) and $NaTp^{Me_2}$ (3.3 g, 10.3 mmol) were placed in a Schlenk flask. THF (125 mL) was added with stirring. The mixture immediately turned from yellow to red/pink. Stirring was continued for 30 min after which the mixture was heated in an oil bath to 80 °C for 2 h with stirring. The mixture was then allowed to stand until the product had settled. The pink supernatant solution was decanted and the solid washed twice more with THF (75 mL). The solid was dried under dynamic vacuum at 80 °C to yield a red/pink powder which was entirely free of iodide. Yield: 3.2 g (89%). X-ray quality crystals can be obtained by the same method as for **1a** or by slow sublimation. IR (KBr, cm^{-1}) ν_{B-H} 2537; MS (EI, 70 eV, 250 °C) *m*/*z* 769 (M^+). Anal. Calcd. for $C_{30}H_{44}N_{12}B_2Yb$: C 46.94; H 5.79; N 21.90; Found: C 45.88, H, 5.54, N 21.53. ^{13}C CPMAS NMR: 11.5 (Me), 13.5 (Me), 105.2 (*C*H), 146.8 (*C*Me), 147.7 (*C*Me).

$Eu(Tp^{Me_2})$, (3a). Europium triflate (500 mg, 0.834 mmol) and KTp^{Me_2} (560 mg, 1.67 mmol) were combined in a Schlenk flask. THF (50 mL) was added and the mixture stirred for 10 min to give a pale yellow turbid solution. After addition of 1% Na/Hg amalgam the solution gradually became orange and a bright orange solid began to separate. After stirring the solution overnight the orange suspension was slurried off the amalgam with a cannula. After allowing the solid to settle the supernatant solution was decanted off and the solid was washed with a further 25 mL THF. The resulting solid was dried in vacuo and purified by sublimation at 250−275 °C (5×10^{-2} mmHg). Yield: 410 mg (66%). IR (KBr, cm^{-1}): ν_{B-H} 2528. Anal. Calcd. for $C_{30}H_{44}N_{12}B_2Eu$: C 48.40; H 5.74; N 22.99; Found: C 48.28, H, 5.90, N 22.53.

3,5-Dimethyl-4-ethylpyrazole. Method A. Addition of acacH (12.2 g, 0.123 mol) to a solution of thallium ethoxide (0.122 mol) in ethanol followed by cooling to −10 °C gave thallium acac as a white powder. The solid was isolated, dried under dynamic vacuum and placed in an ampule with ethyl iodide (74 g, 0.474 mol) and the mixture heated under partial vacuum for 12 h. at ca. 40 °C until the white precipitate of Tlacac had turned to yellow TlI. The mixture was then filtered and the residue extracted with dichloromethane (2×50 mL). The solvent was removed on a rotary evaporator and methanol (50 mL) was added to the residue. Hydrazine hydrate (6.1 g, 0.122 mol) was then added dropwise to the stirred mixture resulting in an exothermic reaction. Once cool, dichloromethane (50 mL) and water (50 mL) were added and the organic layer separated. The aqueous layer was extracted with a further 25 mL of dichloromethane and the combined extracts washed with water (25 mL). After drying over $MgSO_4$, distillation (104−106 °C/6 mmHg) in a short path distillation device gave a yellow oil which slowly crystallized at room temperature. Yield: 6.4 g(42%). ^1H NMR ($CDCl_3$): 2.22 (q, 2H, CH_2CH$_3$); 2.04 (s, 6H, CH$_3$); 0.91 (t, 3H, CH$_2$-CH$_3$). Anal. Calcd. for $C_7H_{12}N_2$: C 67.68, H 9.76; N 22.56; Found: C 67.05, H, 9.99, N 21.89.

Method B. To a suspension of sodium sand (23.0 g, 1 mole) in toluene (1.0 L) was added acacH (110 g, 1.10 mol) dropwise over 30 min. After addition the mixture was refluxed for 30 min until all the sodium had dissolved. After cooling the white solid was filtered on a fritte, washed twice with petrol and dried under dynamic vacuum. The Na(acac) was then mixed with ethyl iodide (530 g, 3.40 mol) and

(40) McNally, S.; Cooper, N. J. In *Experimental Organometallic Chemistry: A Practicum in Synthesis and Characterization*; Wayda, A. L., Darensbourg, M. Y., Eds.; ACS Symposium Series v.357; American Chemical Society: Washington, DC, 1987.
(41) Shriver, D. F.; Drezdzon, M. A. *The Manipulation of Air-Sensitive Compounds*, 2nd ed.; Wiley: New York, 1986.
(42) (a) Namy, J. L.; Girard, P.; Kagan, H. B. *Nouv. J. Chim.* **1981**, *5*, 479. (b) Girard, P.; Namy, J. L.; Kagan, H. B. *J. Am. Chem. Soc.* **1980**, *102*, 2693.
(43) Hamidi, M. E. M.; Pascal, J. L. *Polyhedron* **1994**, *13*, 1787.
(44) Dönges, E. In *Handbook of Peparative Inorganic Chemistry*, 2nd ed.; Brauer, G., Ed.; Academic Press: New York, 1963; Vol. 1, Chapter 16, pp 877−878.
(45) Trofimenko, S.; Calabrese, J. C.; Thompson, J. S. *Inorg. Chem.* **1987**, *26*, 1507.

HMPA (60 mL) in a pressure vessel and heated at 90 °C for 3 days, after which time the solution had turned dark red-brown and a pale yellow precipitate had formed. Water (600 mL) and toluene (750 mL) was added to the mixture and the colored toluene layer separated. This was washed with water (2 × 250 mL) to remove HMPA. Methanol (500 mL) was added and the solution stirred as hydrazine hydrate (50.1 g, 1.0 mmol) was added. A mildly exothermic reaction occurred after which the methanol was removed under reduced pressure and the resulting oil dissolved in toluene (250 mL) and washed with water (2 × 100 mL). Removal of solvent and distillation as before yielded Me_2EtpzH as a yellow crystalline solid. Yield: 66 g (53%).

$KTp^{Me_2,4Et}$. 3,5-dimethyl-4-ethylpyrazole (20.0 g, 0.161 mol) and KBH_4 (1.44 g, 0.0267 mol) were placed in a round-bottomed flask fitted with an air condenser and a nitrogen bubbler. The temperature (monitored by means of a thermometer situated within the apparatus) was steadily increased to 175 °C and maintained at this temperature overnight, after which time hydrogen evolution had ceased. Most of the excess pyrazole was then distilled out of the mixture by attaching a distillation head directly to the flask. Final traces of pyrazole were removed by sublimation onto a liquid nitrogen cooled probe under vacuum to leave pure $KTp^{Me_2,4Et}$. Yield: 9.0 g (79%). IR (KBr) 2440 cm^{-1} (B−H). ^1H NMR (d_6-acetone): 2.25 (q, 6H, CH_2CH_3); 2.13 (s, 9H, CH_3); 2.13 (s, 9H, CH_3); 0.94 (t, 9H, CH_2CH_3). Anal. Calcd. for $C_{21}H_{34}N_6BK$: C, 60.00; H, 8.15; N, 19.99. Found: C, 58.20; H, 8.04; N, 19.30.

$Sm(Tp^{Me_2,4Et})_2$ (1b). To $SmI_2(THF)_{0.65}$ (600 mg, 1.147 mmol) in 50 mL THF was added $KTp^{Me_2,4Et}$ (965 mg, 2.30 mmol) in 50 mL THF over a period of 10 min at −78 °C with stirring. The green solution was allowed to warm slowly to room temperature during which time it changed in color to purple. Stirring was continued for 2 h. The solution was then filtered and the KI residue extracted with THF (3 × 20 mL) until it was virtually colorless. The volume of the filtrate was reduced to 40 mL while keeping the solution above 50 °C to keep the product from crystallizing. Slow cooling to −25 °C gave a purple microcrystalline product which was dried in vacuo at 80 °C. Yield: 670 mg (64%). IR (KBr, cm^{-1}): ν_{B-H} 2527; 1560, 1502(m), 1431(s), 1377, 1361, 1338, 1268, 1231(s), 1167, 1109(s), 1063(m), 997(m), 982-(m), 845(m), 770(m), 720(m), 700(m), 635(m). ^1H NMR (C_6D_6, 298K, δ_{ppm}): −0.04 (s, 18H, Me); 1.71 (t, 18H, Me); 2.72 (q, 12H, CH_2); 18.17 (s, $w_{1/2}$ = 16 Hz, 18H, Me). ^{11}B (C_6D_6, 298K): −49.0. ^{13}C NMR (C_6D_6, 298K): −0.90 (q, 3-Me); 16.5 (q, 4-Me); 18.8 (t, 4-CH_2); 69.4 (s, 3, 4, or 5 C); 94.1 (br q, $w_{1/2}$ = 42 Hz, 5-Me); 123.4 (s, 3, 4, or 5 C);. 209.7 (s, 3, 4, or 5 C). Anal. Calcd. for $C_{42}H_{68}N_{12}B_2Sm$: C 55.24, H 7.52; N 18.41; Found: C 54.81, H, 7.63, N 18.43.

$Yb(Tp^{Me_2,4Et})_2$ (2b). YbI_2 (607 mg, 1.39 mmol) and $KTp^{Me_2,4Et}$ (1171 mg, 2.78 mmol) were mixed in a Schlenk flask and cooled to −78 °C before THF (60 mL) was added. The purple mixture was stirred at −78 °C for 10 min. before being allowed to warm to room temperature to give a purple pink solution and precipitate. Warming in water to 50 °C caused the purple solid to dissolve. The solution was filtered and the volume of THF reduced to 40 mL under reduced pressure. Cooling to −25 °C resulted in the formation of a purple microcrystalline solid which was dried under dynamic vacuum at 80 °C. Yield: 882 mg (68%). IR (KBr, cm^{-1}): ν_{B-H} 2522. UV (THF, nm) 539, 369. ^1H NMR (C_6D_6, 298K): 1.02 (t, 18H, Me); 2.05 (s, 18H, Me); 2.26 (s, 18H, Me); 2.31 (q, 12H, CH_2), 5.1 (br, 2H, BH). ^{11}B (C_6D_6) −8.2. ^{13}C NMR (C_6D_6, 298K): 11.46 (q, 3-Me); 11.55 (q, 5-Me); 15.9 (q, 4-CH_3); 17.1 (t, 4-CH_2); 117 (s, 4-C); 141.3 (s, 3 or 5 C);. 146.4 (s, 5 or 3 C). Anal. Calcd. for $C_{42}H_{68}N_{12}B_2Yb$: C 53.91, H 7.32; N 17.96; Found: C 53.11, H, 7.18, N 18.17.

$Eu(Tp^{Me_2,4Et})_2$ (3b). Europium triflate (557 mg, 0.93 mmol) and $KTp^{Me_2,4Et}$ (782 mg, 1.86 mmol) were combined in a Schlenk flask. THF (50 mL) was added and stirred for 30 min to yield a pale yellow solution and a fine precipitate. Excess 1% Na/Hg amalgam was added and the solution gradually became orange with an orange precipitate. After stirring overnight the reaction mixture was slurried off the amalgam and the solvent removed under reduced pressure. The residue was extracted three times with Et_2O (50 mL, 2 × 25 mL). Removal of solvent yielded a bright orange solid which was purified by sublimation at 250 °C/10^{-2} mmHg. Yield: 460 mg (54%). IR (KBr, cm^{-1}): ν_{B-H} = 2522. UV (THF, nm) 457 (ϵ = 800), 413 (ϵ = 600) Anal. Calcd. for $C_{42}H_{68}N_{12}B_2Eu$: C, 55.14; H, 7.51; N, 18.38; Found: C, 55.26; H, 7.49; N, 18.65.

$Sm(Tp^{Ph})_2$ (1c). A solution of KTp^{Ph} (192 mg, 0.40 mmol) in ca. 15 mL of THF was added dropwise to 2.0 mL of 0.1 M SmI_2 in THF. The mixture was stirred overnight at room temperature, then the THF solvent was removed under vacuum. The residue was extracted with 10 mL of toluene and filtered. Removal of toluene under vacuum yielded **1c** as dark green powder (157 mg, 76%). Diffusion of pentane into the toluene solution afforded dark green crystals suitable for X-ray diffraction. The compound **1c** melted at 180 °C under dynamic vacuum without sublimation. IR (KBr, cm^{-1}) ν_{B-H} 2476; MS (EI, 70 eV, 280 °C) *m*/*z* 1034 (M^+); ^1H NMR (C_6D_6, 25 °C, δ ppm) 15.10 (br s, $w_{1/2}$ = 24 Hz, 12H, *o*-Ph), 8.17 (d, *J* = 7 Hz, 12H, *m*-Ph), 7.70 (d, *J* = 7 Hz, 6H, *p*-Ph), 3.34 (d, *J* = 2 Hz, 6H, pz), −0.22 (d, *J* = 2 Hz, 6H, pz), −3.6 (br s, $w_{1/2}$ = 320 Hz, 2 H, HB); ^{11}B NMR (C_6D_6, 25 °C, δ ppm) −27.75 (br s, $w_{1/2}$ = 170 Hz). Anal. Calcd for $C_{54}H_{44}N_{12}B_2Sm$: C, 62.79; H, 4.26; N, 16.26. Found: C, 62.50; H, 4.69; N, 15.62.

$Yb(Tp^{Ph})_2$ (2c). In a similar fashion, $YbI_2(THF)_{3.5}$ (213 mg) and KTp^{Ph} (302 mg) were mixed and yielded **2c** in 80% yield. Diffusion of pentane into the toluene solution afforded dark red crystals suitable for X-ray diffraction. IR (KBr, cm^{-1}) 2458 (ν_{B-H}); MS (EI, 70 eV, 250 °C) *m*/*z* 1056 (M^+); ^1H NMR (C_6D_6, 25 °C, δ ppm) 7.75 (d, *J* = 2 Hz, 6H, pz), 7.30 (dd, *J* = 7, 1 Hz, 12H, *o*-Ph), 6.68 (tt, *J* = 7, 1 Hz, 6H, *p*-Ph), 6.42 (t, *J* = 7, 12H, *m*-Ph), 6.10 (d, *J* = 2 Hz, 6H, pz), 4.8 (br s, $w_{1/2}$ = 300 Hz, 2H, HB); ^{11}B NMR (C_6D_6, 25 °C, δ ppm) −0.18 (br s). Anal. Calcd for $C_{54}H_{44}N_{12}B_2Sm$: C, 61.44; H, 4.17; N, 15.92. Found: C, 61.67; H, 3.90; N, 15.88.

$Sm(Tp^{Tn})_2$ (1d). A solution of KTp^{Tn} (494 mg, 0.99 mmol) in 10 mL of THF was added dropwise to 5.0 mL of 0.1 M SmI_2 in THF. The mixture was stirred overnight, then the THF was removed under vacuum. The residue was extracted with 20 mL of toluene and filtered. The filtrate was concentrated to ca. 5 mL and stored at −40 °C overnight. Complex **1d** was isolated as a dark green crystalline solid by filtration and drying under vacuum (327 mg, 61%). IR (KBr, cm^{-1}) ν_{B-H} 2434; MS (EI, 70 eV, 250 °C) *m*/*z* 1071 (M^+); ^1H NMR (toluene-d_8, 25 °C, δ ppm) 13.63 (s, 6H, thienyl), 8.12 (d, *J* = 5 Hz, 6H, thienyl), 7.58 (d, *J* = 5 Hz, 6H, thienyl), 3.50 (d, *J* = 2 Hz, 6H, pz), −0.30 (d, *J* = 2 Hz, 6H, pz), −3.14 (br s, 2H, HB); ^{11}B NMR (toluene-d_8, 25 °C, δ ppm) −28.30 (br s). Anal. Calcd for $C_{49}H_{40}N_{12}B_2S_6Sm$: C, 50.29; H, 3.23; N, 14.67. Found: C, 50.14; H, 3.37; N, 14.15.

$Yb(Tp^{Tn})_2$ (2d). In a similar fashion, $YbI_2(THF)_{3.5}$ (106 mg) and KTp^{Tn} (155 mg) were mixed and yielded dark red **2d** in 56% yield. IR (KBr, cm^{-1}) 2453 (ν_{B-H}); MS (EI, 70 eV, 250 °C) *m*/*z*1091 (M^+); ^1H NMR (toluene-d_8, 25 °C, δ ppm) 7.64 (d, *J* = 2 Hz, 6H, pz), 6.93 (dd, *J* = 3, 1 Hz, 6H, thienyl), 6.43 (dd, *J* = 5, 1 Hz, 6H, thienyl), 6.13 (dd, *J* = 5, 3 Hz, 6H, thienyl), 6.12 (d, *J* = 2 Hz, 6H, pz), 5.05 (br s, 2H, HB); ^{11}B NMR (toluene-d_8, 25 °C, δ ppm) −0.21 (br s). Anal. Calcd for $C_{49}H_{40}N_{12}B_2S_6Yb$: C, 46.20; H, 2.95; N, 15.34. Found: C, 46.09; H, 2.88; N, 14.73.

$[Sm(Tp^{Me_2})_2F]$ (1e). Solid PbF_2 (350 mg, 0.14 mmol), which was predried under vacuum overnight at ambient temperature, was added to a stirred slurry of $Sm(Tp^{Me_2})_2$ (0.209 g, 0.28 mmol) in THF in several portions. There was immediate formation of lead and the purple insoluble $Sm(Tp^{Me_2})_2$ gradually disappeared. The resulting mixture was stirred overnight at room temperature. After centrifugation, the colorless supernatant was decanted off and the solvent was removed under vacuum to give $Sm(Tp^{Me_2})_2F$ as a white solid in quantitative yield. The product is pure, as shown by ^1H NMR, but can be further purified by crystallization from THF in 82% recovered yield. This reaction can be carried out in toluene also with a similar yield. IR(KBr, cm^{-1}) ν_{B-H} 2545. ^1H NMR (toluene-d_8, 25 °C, δ_{ppm}): 8.32 (br s, 2H, HB), 5.40 (s, 6H, pz-4H); 3.37 (s, 18H, pz-Me) and −2.08 (s, 18H, Pz-Me). ^{11}B NMR (toluene, 25 °C, δ_{ppm}): −0.03(s). ^{19}F NMR (toluene, 25 °C, δ ppm): −172.26(s). Anal. Calcd for $C_{30}H_{44}N_{12}B_2FSm$: C, 47.18; H, 5.81; N, 22.01 Found: C, 46.84; H, 5.71; N, 21.59.

$[Sm(Tp^{Me_2})_2Cl]$ (1f). $SmCl_3$ (1.15 g, 4.46 mmol) and KTp^{Me_2} (3.00 g, 8.92 mmol) were mixed in a Schlenk tube under nitrogen. THF (60 mL) was added and the mixture stirred overnight (18 h). The very pale yellow slurry was then filtered and the solvent removed under reduced pressure. The resultant off-white solid was extracted with toluene (2 × 40 mL), and the product was obtained by removing the toluene under

Table 2. Average Interatomic Distances (Å) and Angles (deg) and Ranges in the Individual Metrical Parameters for $Sm(Tp^{Me_2})_2F$ (**1e**), $Sm(Tp^{Me_2})_2Cl$ (**1f**), $[Sm(Tp^{Me_2})_2]I$ (**1h**), and $[Sm(Tp^{Me_2})_2][BPh_4]$ (**1j**)

	1e	1f	1h	1j
$Sm-N(pz)_{av}$	2.583(30)	2.563(37)	2.444(12)	2.443(7)
$Sm-N(pz)_{range}$	2.492(10)−2.680(9)	2.467(10)−2.692(11)	2.431(6) and 2.469(6)	2.409(8)−2.479(8)
Sm−X	2.090(7)	2.637(3)		
Sm- - -B	3.60	3.55(2)	3.504(7)	3.51
$N-Sm-N(intra)_{av}$	75.7(16)	76.8(25)	78.0(11)	77.8(15)
$N-Sm-N(intra)_{range}$	70.8(3)−79.3(3)	69.7(3)−84.5(3)	79.1(1) and 75.9(2)	76.7(3)−79.6(3)
$N-B-N_{av}$	111.4(9)	110.8(8)	110.3(5)	110.2(9)
$N-B-N_{range}$	110.6(9)−111.9(11)	107.7(14)−112.9(11)	111.3(5) and 109.8(3)	108.2(9)−111.3(9)
B−Sm−B	144.4	145.7	180	173.2
		Torsion Angles		
$Sm-N-N-B_{av}$	18	17	5.2	6.8
$Sm-N-N-B_{range}$	4.0(11)−26.8(11)	2.0(17)−33.1(14)	7.8(6) and 0.0	0.7(12)−13.9(12)

Table 3. Crystallographic Data

	1a	2a	3a	1b	1c
formula	$C_{30}H_{44}B_2N_{12}Sm$	$C_{30}H_{44}B_2N_{12}Yb$	$C_{30}H_{44}B_2N_{12}Eu$	$C_{50}H_{84}B_2N_{12}O_2Sm$	$C_{54}H_{44}B_2N_{12}Sm$
fw	744.74	767.43	746.35	1057.26	1032.98
space group	$R\bar{3}$ (No.148)	$R\bar{3}$ (No.148)	$R\bar{3}$ (No.148)	$P\bar{1}$ (No.2)	$P\bar{1}$ (No.2)
a, Å	10.612(2)	10.510(3)	10.581(2)	11.089(1)	11.295(2)
b, Å				11.362(1)	11.813(1)
c, Å				12.049(1)	10.851(2)
α, deg	63.30(2)	63.52(2)	63.50(2)	83.951(2)	103.54(1)
β, deg				67.740(2)	112.83(1)
γ, deg				78.066(2)	63.24(1)
V, Å^3	906.8(3)	884.8(4)	906.8(3)	1373.9(2)	1188.4(3)
Z	1	1	1	1	1
ρ_{calc}, g cm^{-3}	1.364	1.440	1.373	1.278	1.443
μ (Mo Kα), mm^{-1}	1.656	2.681	1.775	1.117	1.287
T, °C	20	20	−120	−80	22
R^a	0.030	0.036	0.024	0.046	0.029
$R_w{}^b$	0.064	0.080	0.061	0.105	0.068

	2c	1e	1f	1h	1j
formula	$C_{54}H_{44}B_2N_{12}Yb$	$C_{34}H_{52}B_2FN_{12}OSm$	$C_{30}H_{44}B_2ClN_{12}Sm$	$C_{30}H_{44}B_2IN_{12}Sm$	$C_{64}H_{84}B_3N_{12}O_{2.5}Sm$
fw	1055.67	835.85	780.19	871.64	1244.21
space group	$P\bar{1}$ (No.2)	$P\bar{1}$ (No. 2)	$Pna2_1$ (No.33)	C_2/m (No.12)	$P\bar{1}$ (No.2)
a, Å	10.683(3)	10.715(2)	18.610(3)	16.515(1)	10.045(2)
b, Å	11.029(3)	11.413(2)	10.383(2)	13.050(2)	15.411(3)
c, Å	12.249(3)	18.060(4)	18.634(3)	8.490(1)	21.047(4)
α, deg	63.51(2)	103.84(3)	90	90	90.93(2)
β, deg	82.61(2)	98.27(3)	90	91.77(1)	90.15(2)
γ, deg	66.58(2)	96.89(3)	90	90	98.46(2)
V, Å^3	1183.2(5)	2094.6(7)	3600.6(11)	1828.9(4)	3222.2(11)
Z	1	2	4	2	2
ρ_{calc}, g cm^{-3}	1.482	1.325	1.439	1.583	1.282
μ (Mo Kα), mm^{-1}	2.028	1.447	1.744	2.488	0.964
T, °C	20	20	20	20	20
R^a	0.025	0.067	0.046	0.039	0.065
$R_w{}^b$	0.059	0.190	0.068	0.139	0.132

$^a R = \sum||F_o| - |F_c||/\sum|F_o|$. $^b R_w = [\sum w(F_o^2 - F_c^2)^2/\sum w(F_o^4)]^{1/2}$.

reduced pressure. Pale yellow crystals were grown from a solution made by dissolving 0.5 g of product in hot toluene (10 mL) which was allowed to cool to room temperature before being put in a freezer (−20 °C). Yield: 2.95 g (85%). ^{1}H NMR ($CDCl_3$, 298 K): −0.95 (s, 18H, 3-Me); 3.04 (s, 18H, 5-Me); 5.51 (s, 6H, CH). ^{13}C NMR ($CDCl_3$, 298 K): 11.2 (q, 3 or 5Me); 14.2 (q, 5 or 3Me); 105.4 (d, 4-C); 145.5 (s, 3- or 5-C); 149.4 (s, 5- or 3-C). IR(KBr): 2561 (BH) cm^{-1}. EI/MS: 782 (M^+), 746 ($\{Sm(Tp^{Me_2e})_2\}^+$), 544 ($\{Sm(Tp^{Me_2})(dmpz)\}^+$). Anal. Calcd. for $SmC_{30}H_{44}N_{12}B_2Cl$: C 46.18, H 5.68, N 21.54 Found: C 46.22, H 5.52, N 21.33.

$[Sm(Tp^{Me_2})_2]$Br (1g). $SmBr_3$ (200 mg, 0.51 mmol) was stirred in THF (15 mL) for 15 min. A solution of KTp^{Me_2} (345 mg, 1.03 mmol) dissolved in THF (15 mL) was then added dropwise. The suspended solid dissolved completely by the time half of the ligand had been added after which a fine white precipitate appeared. The reaction mixture was stirred overnight and then allowed to settle. The suspension was filtered and the volume of the filtrate reduced to 5 mL under reduced pressure. The solvent was decanted, and the solid pumped dry. Yield: 0.120 g (15%). IR(KBr): 2561 (BH) cm^{-1} ^{1}H NMR ($CDCl_3$, 298 K): 0.72 (s, 18H, Me); 3.03 (s, 18H, Me); 5.50 (s, 6H, CH). Anal. Calcd for $SmC_{30}H_{44}N_{12}B_2Cl$: C 43.70, H 5.38, N 20.38 Found: C 44.87, H 5.98, N 20.38.

$[Sm(Tp^{Me_2})_2]$I (1h). Method A. A solution of iodine (69 mg, 0.27 mmol) in ca. 5 mL of THF was added dropwise to a slurry of $Sm(Tp^{Me_2})_2$ (400 mg, 0.54 mmol) in 20 mL of THF. A white precipitate formed immediately. The mixture was stirred overnight, the supernatant was decanted off and the precipitate was washed two times with 10 mL of THF. The solid was dried in a vacuum to give **1h** as a white solid (311 mg, 0.35 mmol, 65% yield).

A better yield was obtained using method **B**.

Method B. A solution of $NaTp^{Me_2}$ (370 mg, 1.16 mmol) in THF was added dropwise to a solution of $SmI_3(THF)_3$ (436 mg, 0.58 mmol) in 20 mL of THF. The mixture was stirred overnight and the compound formed was isolated as described in method **A** (380 mg, 0.44 mmol, 75% yield). Single crystals of $Sm(Tp^{Me_2})I$, suitable for an X-ray crystallographic study, could be grown by slow diffusion of *n*-hexane

into a saturated CH_2Cl_2 solution of the complex at room temperature over several weeks. IR(KBr, cm^{-1}) 2563 (BH) cm^{-1}; ^1H NMR ($CDCl_3$, 25 °C, δ_{ppm}); 5.18 (s, 6H, pz-4H), 3.92, −2.48 (s, s; 18H, 18H, pz-Me). Anal. Calcd for $C_{30}H_{44}N_{12}B_2ISm$: C, 41.34; H, 5.09; N, 19.28. Found: C, 41.04; H, 4.83; N, 18.95.

[Sm(Tp^{Me_2})$_2$]I$_3$ (1i). To a purple slurry of Sm(Tp^{Me_2})$_2$ (100 mg, 0.13 mmol) in toluene at room temperature was added a solution of iodine (51 mg, 0.2 mmol). An immediate color change from purple to orange was observed along with the formation of an orange precipitate. The toluene was removed under reduced pressure and the orange solid redissolved in dichloromethane. Addition of diethyl ether resulted in the precipitation of the product. The mixture was allowed to settle for 1 h, the yellow supernatant decanted, and the orange brown powder, **1i**, was dried at room temperature under dynamic vacuum. Yield: 104 mg (71%). IR(KBr, cm^{-1}): 2554 (BH). ^1H NMR ($CDCl_3$, 293 K) −2.57 (s, 18H, Me); 4.03 (s, 18H, Me); 5.21 (s, 6H, CH). ^{13}C NMR ($CDCl_3$, 293 K): 9.3 (q, 3 or 5Me); 15.3 (q, 5 or 3Me); 102.1 (d, C(4)); 144.0 (s, C(3) or C(5)); 147.6 (s, C(5) or C(3)). Anal. Calcd for $C_{36}H_{49}N_{12}B_2SmI_3$: C 32.02, H 3.94, N 14.93; found: C 31.73, H 3.83, N 14.59;

[Sm(Tp^{Me_2})$_2$]BPh$_4$ (1j). Solid $TlBPh_4$ (61 mg, 0.11 mmol) was added in several portions to a slurry of **1a** (84 mg, 0.11 mmol) in 8 mL of THF. A black precipitate of Tl metal formed and the solution become colorless. The mixture was stirred for 2 h and filtered. The filtrate was concentrated to 3 mL and placed at −40 °C overnight. Colorless crystals of **1j** were isolated by filtration and dried under vacuum (60 mg, 50%). Single crystals suitable for X-ray studies were grown by vapor diffusion of hexane into THF solution of **1j**. IR (KBr, cm^{-1}) ν_{B-H} 2560; MS (EI, 70 eV, 200 °C) m/z 745 ($M^+ - BPh_4$); ^1H NMR (THF-d_8, 25 °C, δ ppm) 9.60 (br s, 2H, HB), 7.12 (m, 8H, Ph), 6.70 (m, 8H, Ph), 6.60 (m, 4H, Ph), 5.25 (s, 6H, H-pz), 3.70 (s, 18H, Me-Pz), 3.54 (s, 2H, THF), 1.70 (s, 2H, THF), −2.16 (br, 18H, Me-pz); ^{11}B NMR (THF-d_8, 25 °C, δ ppm) 3.41 (br s, $HBpz_3$), −6.10 (s, BPh_4). Anal. Calcd for $C_{56}H_{68}N_{12}B_3O_{0.5}Sm$: C, 61.17; H, 6.18; N, 15.29. Found: C, 60.91; H, 6.57; N, 15.80.

General Aspects of X-ray Data Collection, Structure Determination, and Refinement. X-ray diffraction were collected using Mo Kα radiation on Syntex P1 (for compounds **1a**, **1e**, **1f**, **1j**, **2a**, and **2c**), Enraf-Nonius CAD4 (**1c** and **1h**), Bruker P4 (**3a**) or Bruker P4/RA/SMART 1000 CCD (**1b**) diffractometers,[46] at ambient room temperature except in the cases of compounds **1b** (−80 °C) and **3a** (−120 °C). For data collections on serial diffractometers, unit cell parameters were obtained from a least-squares refinement of the setting angles of approximately 20 intermediate-angle ($20° \le 2\theta \le 30°$) reflections; for compound **1b**, 3885 reflections from the data collection were used. The data were corrected for absorption through use of a semiempirical method (ψ scans) except in the cases of compounds **1b** and **1c**, where Gaussian integration (after the indexing and measurement of crystal faces) was employed. See Table 3 for a summary of crystal data and X-ray data collection information.

All structures were solved using direct methods (SHELXS-86),[47] and refinement was completed using the program SHELXL-93.[48] Hydrogen atoms were assigned idealized positions based on the geometries of their attached carbon or boron atoms, and were given thermal parameters 20% greater than those of the attached atoms. For compounds **1e** and **1j** the solvent tetrahydrofuran molecules were refined as five-carbon rings in which all single-bond C−C distances were constrained to be equal, and the idealized ring geometry was further imposed by setting the 1,3 distances within the rings to be 163$^1/_3$% of the single-bond distance (to achieve an idealized sp^3 geometry about each ring atom). The final values of $R_1(F)$ (for data with $F_o^2 \ge 2\sigma(F_o^2)$) and $wR_2(R^2)$ (for all independent data) for each compound are found in Table 3; further details regarding structure solution and refinement have been deposited as Supporting Information.

Note Added in Proof. Eu(Tp^{Me_2})$_2$ (**3a**) has also been reported by Christou et al.: Christou, V.; Shipley, C. P.; Capecchi, S.; Dobson, P. J.; Salata, O. V.; Etchells, M. *Adv. Mater.* **1999**, *11*, 533.

Acknowledgment. We are grateful to the Royal Society and the University of London Central Research Fund for support (A.S.) and to EPSRC for studentships to G.H.M. (GR/H31943) and A.C.H. (GR/K11338), to the Natural Sciences and Engineering Research Council of Canada and the University of Alberta (J.T.), to the PRAXIS XXI (2/2.1/QUI/386/74) (N.M.), and to NATO (N.M. and J.T.). Andrea Sella is grateful to Dr. G. Hogarth for access to his drybox. We thank Dr. P. J. Barrie of the ULIRS Solid State NMR service for the spectrum of **2a**, Dr. J. C. Green for recording the photoelectron spectra, Dr. G. Y. Lin for the preparation of Sm(Tp^{Me_2})$_2$F using PbF_2 and Dr. S. Trofimenko for generous gifts of the KTp^{Ph} and KTp^{Tn} ligands.

Supporting Information Available: Tables of X-ray crystallographic data in CIF format for **1a**, **1b**, **1c**, **1e**, **1f**, **1h**, **1j**, **2a**, **2c**, and **3a**. This material is available free of charge via the Internet at http://pubs.acs.org.

IC010325W

(46) Programs for diffractometer operation, data collection, data reduction were those supplied by the diffractometer manufacturers (Syntex, Enraf-Nonius, or Bruker), while the programs used for absorption correction were those of the SHELXTL suite, as supplied by Bruker.

(47) Sheldrick, G. M. *SHELXS-86: Program for the Solution of Crystal Structure*; University of Göttingen: Germany, 1986.

(48) Sheldrick, G. M. *SHELXL-93: Program for the Crystal Structure Refinement*; University of Göttingen: Germany, 1993.